RSC Advances

PAPER

Cite this: *RSC Adv.*, 2015, **5**, 82623

Graphitic carbon nanocage modified electrode for highly sensitive and selective detection of dopamine†

Yi Hong Huang,[a] Jian Hua Chen,*[ab] Xue Sun,[a] Zhen Bo Su,[a] Shi Rong Hu,[a] Wen Weng,[ab] Yang Huang,[a] Wen Bing Wu[a] and Ya San He[a]

Received 30th July 2015
Accepted 10th September 2015

DOI: 10.1039/c5ra15200c

www.rsc.org/advances

In this study, graphitic carbon nanocages (CNCs) with high electrical conductivity were prepared by a solvothermal reaction. Transmission electron microscopy, X-ray photoelectron spectroscopy, Fourier transform infrared spectroscopy and Raman spectroscopy were performed to characterize the morphology and structure of the CNCs. Due to their specific chemical structure, the CNCs provided the modified electrode with a high detecting selectivity as well as sensitivity toward dopamine (DA). Their excellent electrochemical catalytic activityies toward DA were investigated by cyclic voltammetry and differential pulse voltammetry. Under the optimum conditions, the peak current of DA was linear with its concentration in the range of 1–100 μM, and the detection limit was estimated to be 0.18 μM (S/N = 3). This modified glassy carbon electrode showed potential applications in the selective determination of DA due to its attractive merits.

1 Introduction

Nanostructured graphitic carbon materials have attracted intense interest in recent years for their well developed crystalline structures, high electrical conductivity, good thermal stability and excellent oxidation resistance.[1–4] In particular, it has been proposed that carbon materials with a well graphitized structure can lead to higher electrocatalytic activities and improved durability than conventional amorphous carbon when used as catalyst supports.[5,6] Graphitic carbon materials include carbon nanotubes, carbon nanohorns, carbon fibers, carbon nanocoils, graphene, carbon nanocages, and so on. Carbon nanocages (CNCs), 3D nanosized hollow structure particles with a high degree of graphitization and purity, have attracted considerable attention.[7,8] Possessing uniform and tunable mesopore sizes, CNCs have wide applications in many areas, such as the adsorption of small molecules,[9] catalysis,[10] energy storage[11] and membrane fuel cells.[12] However, CNCs have not been used for electroanalysis detection of biological molecules. Moreover, the unique properties of CNCs could enhance the electrocatalytic oxidation of biomolecules by π–π stacking interactions and van der Waal's interactions.[13,14] Nafion is a perfluorinated sulfonated cation exchanger and is composed mainly of a linear backbone of fluorocarbon chains and ethyl ether pendant groups with sulfonic cation exchange sites. Up to date, Nafion still functions as the best performing cation exchange membrane owing to its mechanical strength, and high chemical and thermal stability.[15] Moreover, Nafion can reduce or avoid the effect of electrode fouling, which is a common problem in electrochemical determination of phenolic compounds.[16,17] Therefore, this invited us to examine, systematically, the role of CNCs as a fast electron transfer mediator on the electrochemical detection of biomolecules.

Dopamine (DA, 3,4-dihydroxyphenyl ethylamine) is an important neurotransmitter widely distributed in the mammalian central nervous system for message transfer.[18,19] It plays a crucial role in the functioning of the central nervous, cardiovascular, renal and hormonal systems, as well as emotional processes in human metabolism. In addition, DA makes a significant contribution to the neurophysiological control of arousal and attention, initiation of movement, perception, motivation and emotion. Abnormal levels of DA can cause brain disorders such as schizophrenia and Parkinson's disease.[20–23] Many techniques have been employed to detect DA, such as colorimetry,[24] electrophoresis,[25] spectrophotometry,[26] chromatography,[27] chemiluminescence,[28] and spectro-fluorimetry.[29] However, these techniques are complicated, expensive and time consuming. To overcome these shortcomings, electrochemical methods have been employed for quantitative determination of DA *in vivo*/*vitro* in clinical and pathological research due to their simplicity, fast responses, relatively cheap costs and low power requirements.[30]

[a]*College of Chemistry and Environmental, Minnan Normal University, Zhangzhou 363000, China. E-mail: jhchen73@126.com; Fax: +86-596-2520035; Tel: +86-596-2591445*

[b]*Fujian Province University Key Laboratory of Modern Analytical Science and Separation Technology, Minnan Normal University, Zhangzhou 363000, China*

† Electronic supplementary information (ESI) available. See DOI: 10.1039/c5ra15200c

In this study, CNCs with high conductivity were obtained by a hydrothermal synthesis sacrifice template method. Then a well-dispersed solution containing CNCs and Nafion was prepared, and subsequently casted onto a glassy carbon electrode (GCE) to achieve a CNCs/Nafion hybrid modified electrode. CNCs/Nafion/GCE was constructed for the determination of DA in the presence of its major interferents ascorbic acid (AA) and uric acid (UA), with excellent selectivity, broad linear range and a low detection limit. It may be the case that the aromatic π–π stacking and electrostatic attraction between the positively charged DA and negatively charged CNCs/Nafion can accelerate the electron transfer, while reducing the oxidation of AA and UA on the CNCs/Nafion/GCE.[31] Furthermore, satisfactory results were obtained when practical application was investigated in a DA hydrochloride injection using a standard addition method.

2 Experimental

2.1 Chemicals

DA, AA and UA were obtained from Sinopharm Chemical Reagent Co. Ltd (Shanghai, China). The DA hydrochloride injection was obtained from Shanghai Harvest Pharmaceutical Co. Ltd (Shanghai, China). Ferrous oxalate was purchased from Aladdin (Shanghai, China). All chemicals were of analytical reagent grade and used without further purification. All the aqueous solutions were prepared with distilled water (18.2 MΩ). The DA solution was prepared with double distilled water. Working solutions were prepared by diluting in 0.2 M phosphate buffer solution (PBS, pH = 6.0) before use. Both the standard solution and buffer solution were kept in a 4 °C refrigerator.

2.2 Apparatus

Electrochemical measurements were performed on a CHI 650D electrochemical workstation (Shanghai Chenhua Instruments Co., China). The conventional three-electrode system consisted of a KCl saturated Ag/AgCl electrode (reference electrode), a Pt wire electrode (auxiliary electrode), and a bare or modified GCE with 3.0 mm diameter (working electrode). Cyclic voltammetry (CV) (initial potential: −0.2 V; high potential: 0.6 V; low potential: −0.2 V; scan rate 100 mV s^{-1}) and differential pulse voltammetry (DPV) (initial potential: −0.2 V; final potential: 0.6 V; incremental potential: 0.004 V; amplitude: 0.05 V; pulse width: 0.05 s; sampling width: 0.0167; pulse period: 0.5 s; quiet time: 2 s) were carried out at room temperature. Adjustment of pH was carried out using a Mettler Toledo FE-20 pH meter (Shanghai, China).

2.3 Characterization techniques

Determination of the microstructure of the CNCs was performed on a transmission electron microscope (TEM, FEI company, FEI Tecnai G2-20, USA). The Raman spectrum was recorded at ambient temperature on a LABRAMHR confocal laser MicroRaman spectrometer with an argon-ion laser at an excitation wavelength of 525 nm (Raman, Renishaw Invia). The X-ray photoelectron spectroscopy (XPS) was conducted on a Thermo Scientific K-Alpha electron energy spectrometer using Al Kα (1486.6 eV) as the X-ray excitation source, and the binding energy calibration was based on C 1s at 284.8 eV. The Fourier transform infrared (FT-IR) spectrum was recorded on a Thermo NICOLET iS 10 (Thermo Fisher Scientific, America) using KBr pressed disks. The surface morphology of the CNC film on GCE was observed with atomic force microscopy (AFM, CSPM5500, China).

2.4 Preparation of the CNCs/Nafion/GCE

Prior to surface modification, the surface of the GCE was polished to a mirror-like surface using 1.0 μm, 0.3 μm and 0.05 μm alumina slurry respectively, then successively sonicated in distilled water, ethanol and distilled water for 5 min and dried with N_2 before use.

CNCs were prepared according to Li's methods.[32] Briefly, 15 mL ethanol and 1.5 g ferrous oxalate were added to a 20 mL stainless-steel autoclave and heated at 550 °C for 12 h. Then the dark precipitates were collected and successively washed with absolute ethanol, hydrochloric acid and distilled water several times, followed by drying in a vacuum at 60 °C for 5 h for further use.

3 mg of CNCs was added into the mixed solution containing 0.1 mL Nafion and 0.9 mL ethanol, followed by ultrasonication for 20 min to form a homogeneous CNC dispersion. The CNCs/Nafion/GCE was obtained by casting 5 μL of CNCs/Nafion solution onto the surface of the GCE and drying at room temperature.

3 Results and discussion

3.1 Characterization of the CNCs

The TEM image (Fig. 1A) displays the uniform tetragonal projected shapes and hollow structures of the CNCs. Most of the CNCs have a quadrangular configuration, which can be further proved by the HRTEM image (Fig. 1B).

Fig. 2A shows the XPS patterns of the CNCs. It provides direct evidence for the elemental composition of the CNCs. The full scan of the CNCs presented the binding energies of C 1s (284.77 eV) and O 1s (532.82 eV), which indicated that the main chemical element components of the CNCs were C and O. In addition, the C 1s spectrum of the CNCs, as shown in Fig. 2B, was split into three peaks, which demonstrated that three different types of carbon were present in the CNCs: C1 at 284.77

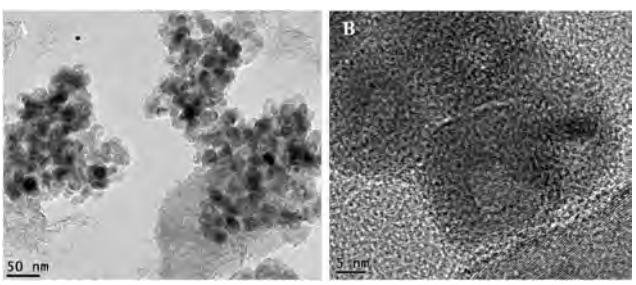

Fig. 1 TEM (A) and HRTEM (B) images of the CNCs.

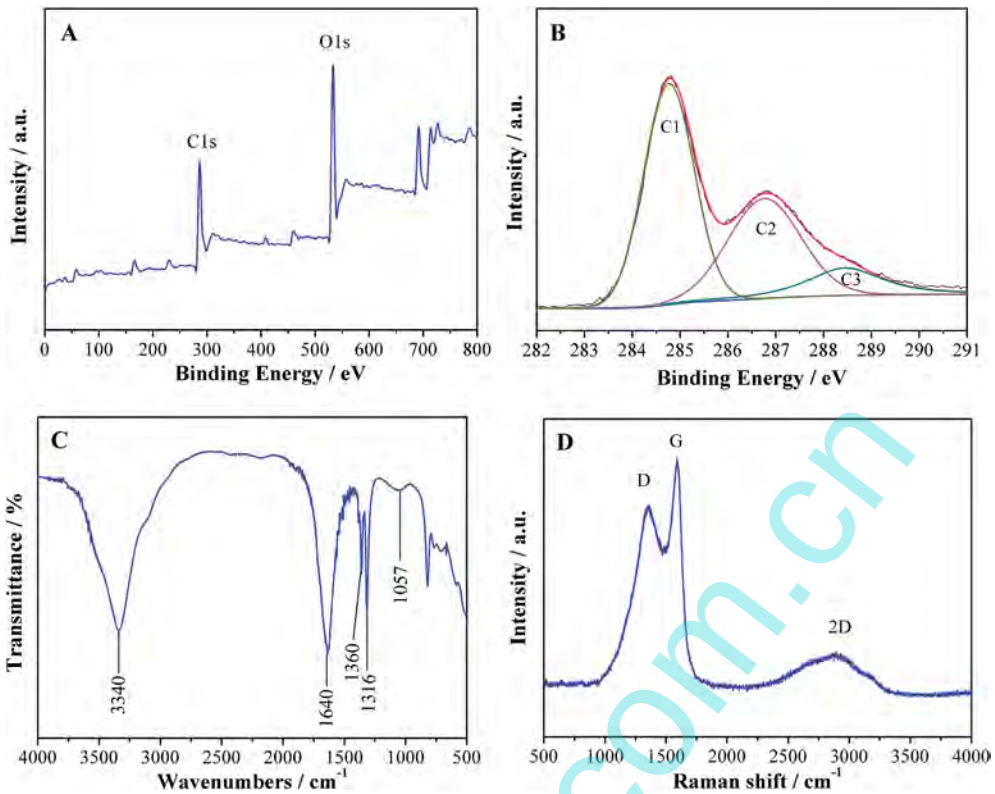

Fig. 2 XPS full scan (A), C 1s spectrum (B), FT-IR spectrum (C), and Raman spectrum (D) of CNCs.

eV corresponded to non-oxygenated ring carbon, C2 at 286.79 eV was assigned to C–O, and C3 at 288.84 eV was in accordance with C═O.

The FT-IR spectrum was used to analyze the major functional groups of the CNCs. As displayed in Fig. 2C, there were several obvious peaks approximately located at 3340 cm^{-1}, 1640 cm^{-1}, 1360 cm^{-1}, 1316 cm^{-1} and 1057 cm^{-1}, which were assigned to O–H stretching vibrations, C═O stretching vibrations, O–H deformation vibrations, C–O–C stretching vibrations and C–O bending vibrations, respectively. These results were consistent with the XPS. In addition, Raman spectroscopy was used for qualitative and quantitative analysis of the CNCs, which is shown in Fig. 2D. The D band at 1350.60 cm^{-1} was associated with the defects, curved sheets and dangling bonds in the carbon structures.[33] The G band at 1595.55 cm^{-1} could correspond to the vibration of sp^2 hybridized carbon atoms in a 2D hexagonal lattice.[34] The disorder degree in graphite layers was estimated by the ratio of the intensity of the D band to G band (I_D/I_G), and the I_D/I_G value for the CNCs was calculated to be 0.83 from Fig. 2D. The I_D/I_G intensity ratio of the CNCs indicated carbon layers of the CNCs being mainly disordered, which is consistent with the reported literature.[32] Moreover, the CNC materials also exhibited a strong Raman band at 2D which appeared at about 2701 cm^{-1}. This can be attributed to second-order bands of overtones of graphitic lattice vibration modes.[35,36]

From Fig. S1,† it can be observed that the XRD pattern of the CNCs displayed the appearance of two prominent diffraction peaks at 21.6° and 43.2°, corresponding with the (002) and (101) reflections of hexagonal graphite turbostratic carbon, respectively (JCPDS card no. 41-1487). This indicated low crystallinity or disordered graphite of the CNCs has formed.

The morphologies of the GCE, Nafion/GCE and CNCs/Nafion/GCE were investigated by AFM (317 × 311 nm^2 scope). Fig. 3 displays the typical topographic (a) and three dimensional (b) images of the GCE (A), Nafion/GCE (B) and CNCs/Nafion/GCE (C). The dark and light areas represent the lower and higher regions on the surface, respectively. A relatively flat and smooth surface can be observed on the GCE and Nafion/GCE. However, the surface of the CNC/Nafion/GCE was rugged after being modified with the CNCs. The surface roughnesses (S_a-roughness average) of the bare GCE, Nafion/GCE and CNCs/Nafion/GCE were calculated to be 0.608, 0.785 and 1.75 nm, which indicates that the CNCs had been anchored on the GCE and the surface effect of the electrode interface has been improved.

3.2 Electrochemical behavior of DA on the modified electrodes

The electrochemical properties of the CNCs were examined with CV. As shown in Fig. 4, peaks at 0.323 V and 0.180 V represented the redox of DA on the bare GCE. Strong peaks were observed at 0.484 V and 0.020 V on the Nafion/GCE. The CNCs/Nafion/GCE showed the strongest and quasi-reversible redox peaks of DA at 0.285 V and 0.183 V, and a peak-to-peak separation of about 102 mV revealed a fast electron-transfer process.[37] The characteristic oxidation peak of DA increased remarkably on the CNCs/

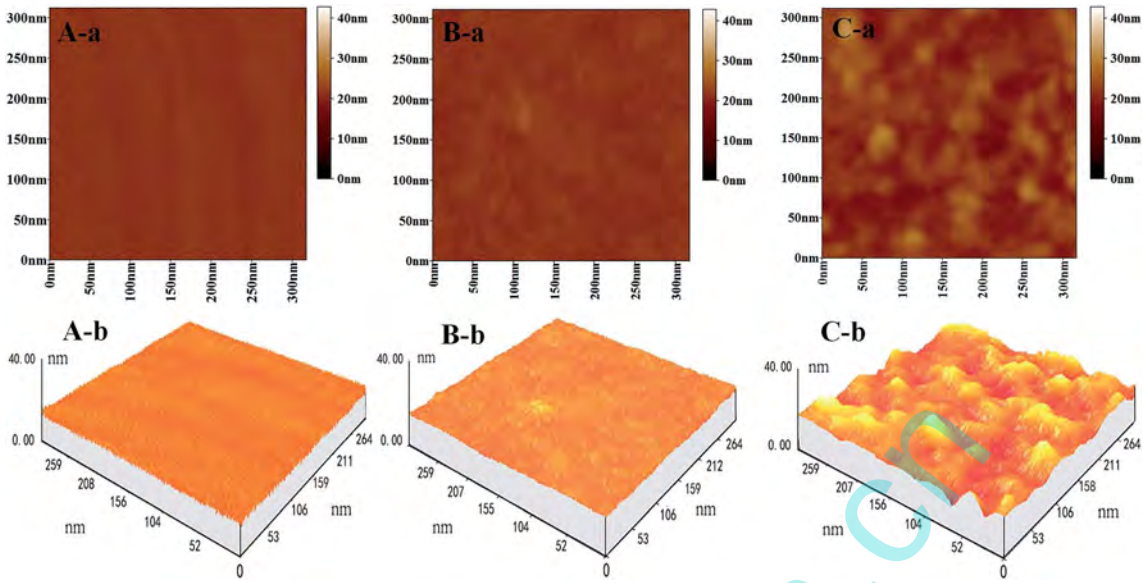

Fig. 3 AFM (a) and 3D (b) images of the bare GCE (A), Nafion/GCE (B) and CNCs/Nafion/GCE (C).

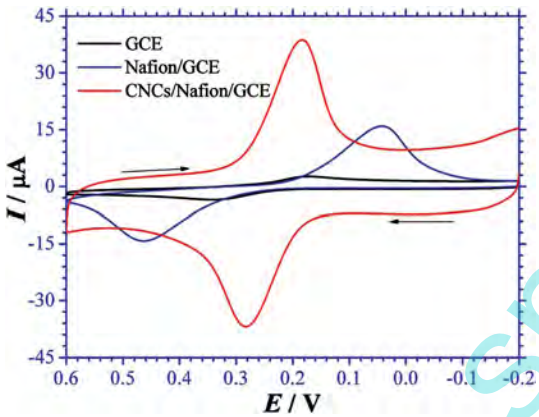

Fig. 4 CVs of 100 μM DA in 0.1 M PBS with pH 6.0 on the bare GCE, Nafion/GCE and CNCs/Nafion/GCE. Scan rate: 100 mV s^{-1}.

Nafion/GCE compared with that of the bare GCE and Nafion/GCE at pH 6.0. The mechanism of the redox reaction of DA on the CNCs/Nafion/GCE is presented in Scheme 1. The increase of the peak current could be attributed to the π–π stacking interaction between the π-conjugation of the CNCs and the phenyl moiety of DA.[38,39] Nafion film with negative charge was an efficient barrier to the negatively charged interfering compounds such as AA and UA, and conduced the accumulation of positively charged DA at the Nafion film.[40,41] Additionally, CNCs, with their outstanding electric conductivity, could accelerate electron transfer on the electrode surface and amplify the electrochemical signals, and thus show enhanced sensitivity toward DA. In this paper, the effect of the concentration of the CNCs on the DA signal was also investigated by DPV. The result is shown in Fig. S2.† It demonstrates that the signal of the peak current gradually increased with increasing the amount of the components. In addition, electrochemical impedance spectroscopy (EIS) was employed to measure the electron transfer properties of different modified electrodes. The electron transfer kinetics of $[Fe(CN)_6]^{3-/4-}$ at different electrodes is provided in Fig. S3.† On the basis of a typical Nyquist plot, EIS consists of two parts: a linear part at low frequency and semicircle part at high frequency. The linear part is a diffusion controlled process, and the semicircle part is in conformity to the electron transfer resistance (R_{et}).[42,43] It can be obviously observed that CNCs/Nafion showed a lower R_{et} value than Nafion/GCE and GCE. This demonstrated that CNCs/Nafion exhibited a higher conductivity and faster electron transfer process.

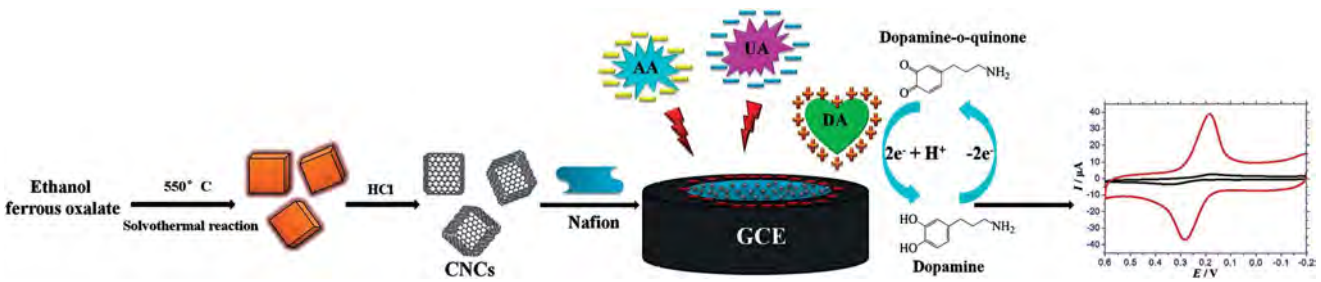

Scheme 1 Schematic illustration of the preparation procedure of the CNCs and the electrochemical effect of the CNCs/Nafion/GCE on DA.

3.3 pH effect

The effect of pH on the detection of DA by the CNCs/Nafion/GCE was checked by CV. As shown in Fig. 5A, the oxidation and reduction peak currents of DA gradually increase with pH from 4.0 to 6.0, but gradually decrease with pH from 6.0 to 9.0. Therefore, this modified electrode had a maximum peak current of DA at pH 6.0. Moreover, it can be seen that the oxidation and reduction peak potentials shift negatively with increasing pH from 4.0 to 9.0 for DA. In addition, a good linear relationship (Fig. 5B) between the oxidation peak potential (E_{pa}) and pH. The linear regression equation could be expressed as E_{pa} (V) = −0.0464 pH + 0.5595 (R = 0.9950). A slope value of 46.4 mV pH^{-1} was calculated from the regression equation denoting that the electron transfer was accompanied by an equal number of protons, which was consistent with that reported in the literature.[44]

3.4 Effect of scan rate

In order to better understand the electrochemical mechanism of DA on the surface of the CNCs/Nafion/GCE, the effect of scan rate was also investigated. Fig. 6A displays the CV curves of the CNCs/Nafion/GCE at different scan rates. The cathodic and anodic peak currents of DA increased linearly with the square root of the scan rate in the range of 0.01–0.25 V s^{-1}. Fig. 6B shows the calibration curve of the response peak current to the square root of the scan rate. The linear regression equation for the anode peak current (I_{pa}) is I_{pa} (μA) = $-78.34\nu^{1/2}$ (V$^{1/2}$ s$^{-1/2}$) + 5.326 (R = 0.9965) and the cathode peak current (I_{pc}) is I_{pc} (μA) = $95.31\nu^{1/2}$ (V$^{1/2}$ s$^{-1/2}$) − 6.090 (R = 0.9987). The peak current shows a linear relationship with the square root of the scan rate, indicating that the electrochemical reaction was a reversible and diffusion controlled electrochemical process.

3.5 Electrochemical detection of DA

Due to the better current sensitivity and resolution than CV, a quantitative analysis of DA was performed by DPV.[45] Fig. 7 presents DPV of different concentrations of DA on the CNCs/Nafion/GCE. Under the optimal conditions, the sharp and well-defined oxidation peak current of DA increased with concentration. A good linear relationship between the oxidation peak current of DA and concentration was presented in the range of 1–100 μM. The linear regression equation was expressed as I (μA) = $-0.3516C_{DA}$ (μM) − 1.367 (R = 0.9902). Moreover, based on 3σ (where σ is the standard deviation of a blank solution, n = 9), the detection limit was estimated to be 0.18 μM. The DA determination results of the CNCs and other carbon-based nanomaterials are exemplified in Table 1. This suggests that the CNCs/Nafion/GCE showed an excellent selectivity for DA.

3.6 Interference effects

The major interference effects for DA detection are from AA and UA since they are oxidized at a similar potential and measurement was performed by DPV methods. The modified electrode showed no interference from AA and UA for detecting DA in this work, which is displayed in Fig. S4.† The reason for this was also discussed in Scheme 1. The CNCs with a graphite-like structure can form π–π stacking interactions between the π-conjugation of the CNCs and the phenyl moiety of DA, but not AA or UA. At the physiological pH of 7.4, AA (pK_a = 4.10) and UA (pK_a = 5.75) exist in an anionic form, while DA is in a cationic form (pK_b = 8.87). Specifically, Nafion is a cation-exchange polymer and an excellent surfactant that is negatively charged and can remove anionic interference. The Nafion coating acts as a covering to immobilize the CNC film on the GCE surface, as well as an interferent barrier.[51]

3.7 Real sample analyses

DA is stable in acidic media.[52] To evaluate the applicability of the CNCs/Nafion/GCE, the DA hydrochloride samples were freshly prepared by diluting stock solution with PBS (0.1 M, pH 6.0), and were injected for detection *via* a standard addition method. No other pretreatment process was performed. The summarized results for the real sample analyses are given in Table 2. Satisfactory results for the recoveries in the range of 99.10–102.5% can be obtained. This indicated that the proposed electrode could be efficiently used for the determination of DA.

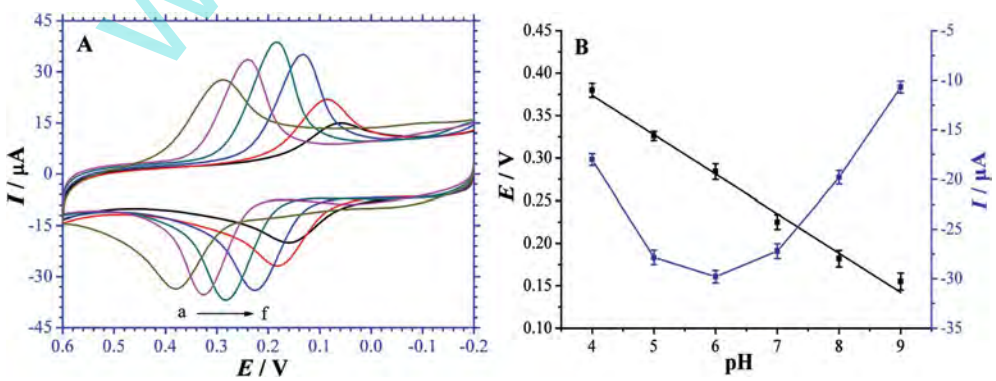

Fig. 5 (A) CVs of 100 μM DA on the CNCs/Nafion/GCE in 0.1 M PBS with various pH values (a–f: 4.0, 5.0, 6.0, 7.0, 8.0, 9.0). (B) Peak potential and peak current *vs.* pH. Scan rate: 100 mV s^{-1}.

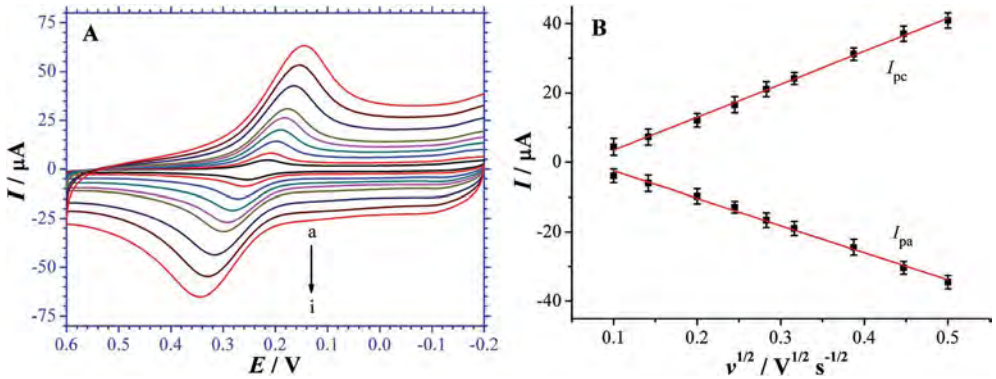

Fig. 6 (A) CVs of 100 μM DA in the 0.1 M PBS with different scan rates (a–i: 0.01, 0.02, 0.04, 0.06, 0.08, 0.10, 0.15, 0.20, 0.25 V s^{-1}). (B) Peak potential and peak current *vs.* the square root of the scan rate.

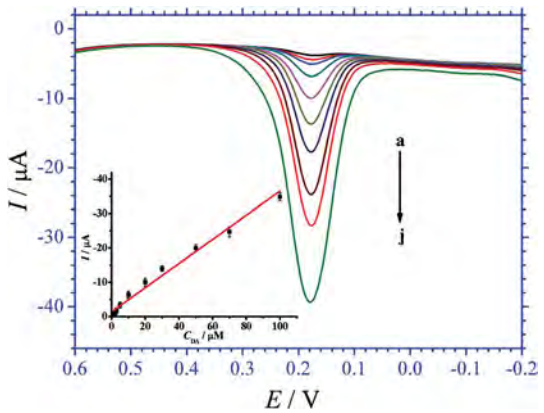

Fig. 7 DPV curves from the CNCs/Nafion/GCE with different concentrations of DA (from a to j: 1, 2, 3, 5, 10, 20, 30, 50, 70, 100 μM). Inset: peak current response *vs.* DA concentration.

Table 1 Comparison of the modified electrode with previously reported carbon nanomaterial modified electrodes for DA

Materials	Detection limit (μM)	Linear range (μM)	References
Graphene	2.64	4–100	39
GO	0.27	1–15	46
ECNF[a]	0.04	0.04–5.6	47
SWCNT[b]	0.06	0.2–3.8	48
MWCNT[c]	0.8	3–200	49
MWCNT/Nafion	0.08	0.1–80	50
CNCs/Nafion	0.18	1–100	This work

[a] Electrospun carbon nanofibers. [b] Single-walled carbon nanotubes. [c] Multi-walled carbon nanotubes.

3.8 Stability research

In this paper, the stability of this method was also researched. CV response for 100 μM DA on the CNCs/Nafion/GCE in 0.1 M PBS with pH 6.0 is shown in Fig. 8. The electrode was put into a vacuum drying oven at 25 °C, and the DA samples were determined every four days. It was clearly observed that the redox peak potential and current remained stable. The relative

Table 2 Recoveries of DA in the DA hydrochloride injection samples on the CNCs/Nafion/GCE *via* a standard addition method ($n = 5$)

DA injection (μM)	Added (μM)	Found (μM)	Recovery (%)	RSD (%)
2	0	2.05	102.5	2.55
2	8	9.91	99.10	1.97
2	28	30.06	100.2	2.71
2	48	49.62	99.24	2.28

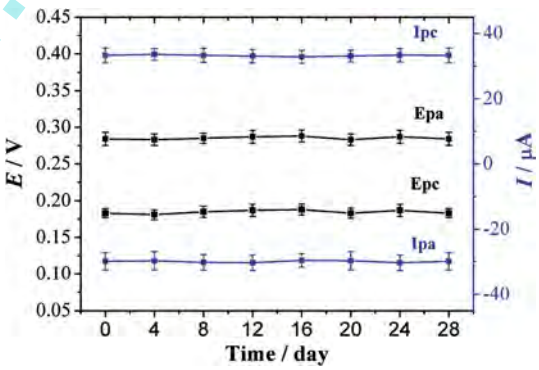

Fig. 8 The stability of the CNCs/Nafion/GCE in 0.1 M PBS with pH 6.0 for detection of 100 μM DA.

standard deviations (RSDs) of I_{pc}, E_{pa}, I_{pa} and E_{pc} for DA were calculated to be 0.45%, 1.86%, 2.74% and 1.63% respectively. Therefore, the modified electrode has an excellent stability and reproducibility for DA detection.

4 Conclusions

In conclusion, we have successfully constructed a novel DA biosensor by covering the surface of the GCE with a CNCs/Nafion thin film. With a simple template method, the CNCs with a porous graphitized carbon core/shell structure were prepared. The Nafion, a perfluorinated sulfonated cation exchanger, could be used for dispersing CNCs in ethanol solution well, and help in the formation of a stable and uniform

CNCs/Nafion thin film on the GCE surface. In comparison to the GCE and Nafion/GCE, the CNCs/Nafion/GCE had distinguished electrocatalytic activity toward the oxidation of DA. As expected, a remarkable sensitivity, low limit of detection (0.18 μM) as well as a linear response in a range of 1–100 μM can be achieved. In addition, this study also implies that the as-prepared CNCs/Nafion/GCE is quite suitable for determining not only DA but also similar biomolecules in analytical applications.

Acknowledgements

The authors would like to acknowledge the financial support of this work from National Natural Science Foundation of China (No. 21076174), National Natural Science Foundation of China (No. 21175115), National Natural Science Foundation of Fujian (2012J06005 and 2014J01051), and the Science and Technology Key Project of Fujian (2013H0053). The authors also thank the anonymous referees for comments on this manuscript.

References

1 J. Wang, Y. Zhao and J. Niu, *J. Mater. Chem.*, 2007, **17**, 2251–2256.
2 A. H. Lu, W. C. Li, E. L. Salabas, B. Spliethoff and F. Schüth, *Chem. Mater.*, 2006, **18**, 2086–2094.
3 J. Yuan, C. Giordano and M. Antonietti, *Chem. Mater.*, 2010, **22**, 5003–5012.
4 C. Wang, D. Ma and X. Bao, *J. Phys. Chem. C*, 2008, **112**, 17596–17602.
5 M. Sevilla, G. Lota and A. B. Fuertes, *J. Power Sources*, 2007, **171**, 546–551.
6 M. Sevilla, C. S. Martínez-de Lecea, T. Valdés-Solís, E. Morallón and A. B. Fuertes, *Phys. Chem. Chem. Phys.*, 2008, **10**, 1433–1442.
7 S. Teng, X. Wang, B. Xia and J. Wang, *J. Power Sources*, 2010, **195**, 1065–1070.
8 X. W. D. Lou, L. A. Archer and Z. Yang, *Adv. Mater.*, 2008, **20**, 3987–4019.
9 A. Vinu, M. Miyahara, V. Sivamurugan, T. Mori and K. Ariga, *J. Mater. Chem.*, 2005, **15**, 5122–5127.
10 Y. Li, C. Zhou, X. Xie, G. Shi and L. Qu, *Carbon*, 2010, **48**, 4190–4196.
11 O. V. Pupysheva, A. A. Farajian and B. I. Yakobson, *Nano Lett.*, 2007, **8**, 767–774.
12 Z. M. Sheng and J. N. Wang, *Adv. Mater. Adv. Mater.*, 2008, **20**, 1071–1075.
13 S. Chen, J. Bi, Y. Zhao, L. Yang, C. Zhang, Y. Ma, Q. Wu, X. Wang and Z. Hu, *Adv. Mater.*, 2012, **24**, 5593–5597.
14 Y. H. Huang, J. H. Chen, X. Sun, Z. B. Su, H. T. Xing, S. R. Hu, W. Weng, H. X. Guo, W. B. Wu and Y. S. He, *Sens. Actuators, B*, 2015, **212**, 165–173.
15 A. Babaei and A. R. Taheri, *Sens. Actuators, B*, 2013, **176**, 543–551.
16 X. Yang, J. Kirsch, E. V. Olsen, J. W. Fergus and A. L. Simonian, *Sens. Actuators, B*, 2013, **177**, 659–667.
17 X. Yang, J. Kirsch, J. Fergus and A. Simonian, *Electrochim. Acta*, 2013, **94**, 259–268.
18 H. Ghadimi, M. R. Mahmoudian and W. J. Basirun, *RSC Adv.*, 2015, **5**, 39366–39374.
19 G. Jiang, T. Jiang, H. Zhou, J. Yao and X. Kong, *RSC Adv.*, 2015, **5**, 9064–9068.
20 X. Wang, Z. You, H. Sha, Y. Cheng, H. Zhu and W. Sun, *Talanta*, 2014, **128**, 373–378.
21 S. Cheemalapati, S. Palanisamy, V. Mani and S. M. Chen, *Talanta*, 2013, **117**, 297–304.
22 J. Kim, J. Auerbach, J. Gómez, I. Velasco, D. Gavin, N. Lumelsky, S. Lee, J. Nguyen, R. Pernaute, K. Bankiewicz and R. McKay, *Nature*, 2002, **418**, 50–56.
23 R. Wightman, L. May and A. Michael, *Anal. Chem.*, 1988, **60**, 769A–793A.
24 J. J. Feng, H. Guo, Y. F. Li, Y. H. Wang, W. Y. Chen and A. J. Wang, *ACS Appl. Mater. Interfaces*, 2013, **5**, 1226–1231.
25 X. Wang, Y. Ma, X. Yao, J. Wang and M. Yin, *RSC Adv.*, 2013, **3**, 24605–24611.
26 A. Abbaspour, A. Khajehzadeha and A. Ghaffarinejad, *Analyst*, 2009, **134**, 1692–1698.
27 Y. Zhou, H. Yan, Q. Xie, S. Huang, J. Liu, Z. Li, M. Ma and S. Yao, *Analyst*, 2013, **138**, 7246–7253.
28 L. Zhang, Y. Cheng, J. Lei, Y. Liu, Q. Hao and H. Ju, *Anal. Chem.*, 2013, **85**, 8001–8007.
29 H. Y. Wang, Y. Sun and B. Tang, *Talanta*, 2002, **57**, 899–907.
30 B. Li, Y. Zhou, W. Wu, M. Liu, S. Mei, Y. Zhou and T. Jing, *Biosens. Bioelectron.*, 2015, **67**, 121–128.
31 L. Wu, L. Feng, J. Ren and X. Qu, *Biosens. Bioelectron.*, 2012, **34**, 47–52.
32 G. Li, H. Yu, L. Xu, Q. Ma, C. Chen, Q. Hao and Y. Qian, *Nanoscale*, 2011, **3**, 3251–3257.
33 K. Wang, Z. Li, Y. Wang, H. Liu, J. Chen, J. Holmes and H. Zhou, *J. Mater. Chem.*, 2010, **20**, 9748–9753.
34 Y. Tan, C. Xu, G. Chen, Z. Liu, M. Ma, Q. Xie, N. Zheng and S. Yao, *ACS Appl. Mater. Interfaces*, 2013, **5**, 2241–2248.
35 M. A. Pimenta, G. Dresselhaus, M. S. Dresselhaus, L. G. Cançado, A. Jorio and R. Saito, *Phys. Chem. Chem. Phys.*, 2007, **9**, 1276–1291.
36 A. Sadezky, H. Muckenhuber, H. Grothe, R. Niessner and U. Pöschl, *Carbon*, 2005, **43**, 1731–1742.
37 K. Liu, J. Wei and C. Wang, *Electrochim. Acta*, 2011, **56**, 5189–5194.
38 Y. Wang, Y. Li, L. Tang, J. Lu and J. Li, *Electrochem. Commun.*, 2009, **11**, 889–892.
39 H. Zhang, Q. Huang, Y. Huang, F. Li, W. Zhang, C. Wei, J. Chen, P. Dai, L. Huang, Z. Huang, L. Kang, S. Hu and A. Hao, *Electrochim. Acta*, 2014, **142**, 125–131.
40 N. F. Atta and M. F. El-Kady, *Sens. Actuators, B*, 2010, **145**, 299–310.
41 L. Dennany, M. Gerlach, S. O'Carroll, T. E. Keyes, R. J. Forster and P. Bertoncello, *J. Mater. Chem.*, 2011, **21**, 13984–13990.
42 J. Li, Y. Shen, Y. Zhang and Y. Liu, *Chem. Commun.*, 2005, 360–362.
43 H. Zhang, Y. Huang, S. Hu, Q. Huang, C. Wei, W. Zhang, W. Yang, P. Dong and A. Hao, *Electrochim. Acta*, 2015, **176**, 28–35.
44 Z. Herrastia, F. Martíneza and E. Baldrich, *Sens. Actuators, B*, 2014, **203**, 891–898.

45 R. M. A. Tehrani, H. Ghadimi and S. A. Ghani, *Sens. Actuators, B*, 2013, **177**, 612–619.
46 F. Gao, X. Cai, X. Wang, C. Gao, S. Liu, F. Gao and Q. Wang, *Sens. Actuators, B*, 2013, **186**, 380–387.
47 Y. Liu, J. Huang, H. Hou and T. You, *Electrochem. Commun.*, 2008, **10**, 1431–1434.
48 S. Zhu, H. Li, W. Niu and G. Xu, *Biosens. Bioelectron.*, 2009, **25**, 940–943.
49 Z. A. Alothman, N. Bukhari, S. M. Wabaidur and S. Haider, *Sens. Actuators, B*, 2010, **146**, 314–320.
50 S. Shahrokhian and H. R. Zare-Mehrjardi, *Electrochim. Acta*, 2007, **52**, 6310–6317.
51 S. Yuan and S. Hu, *Electrochim. Acta*, 2004, **49**, 4287–4293.
52 B. Wu, C. Miao, L. Yu, Z. Wang, C. Huang and N. Jia, *Sens. Actuators, B*, 2014, **195**, 22–27.